Kinetics and Mechanism of the Reaction of Cyanide[1] with Molybdenum Nitrogenase from *Azotobacter vinelandii*†

David J. Lowe,‡ Karl Fisher,‡ Roger N. F. Thorneley,‡ Stephen A. Vaughn,§,∥ and Barbara K. Burgess*,§

Department of Molecular Biology and Biochemistry, University of California, Irvine, California 92717, and Agriculture Food Research Council Institute of Plant Science Research, University of Sussex, Brighton BN1 9RQ, United Kingdom

Received March 9, 1989; Revised Manuscript Received June 22, 1989

ABSTRACT: The steady-state kinetic behavior of the six-electron reduction of N_2 by nitrogenase is known to differ markedly from the six-electron reduction of cyanide in two ways. First, on extrapolation to infinite concentration of cyanide, the H_2 evolution reaction is almost completely suppressed whereas at extrapolated infinite concentration of N_2, H_2 evolution continues. Second, as the ratio of the Fe protein to the MoFe protein increases, the reduction of N_2 is favored over H_2 evolution, whereas the reduction of cyanide becomes less favored relative to H_2 evolution. We have extended these steady-state experiments with *Azotobacter vinelandii* nitrogenase to include a third observation, that the six-electron reduction of N_2 is favored over H_2 evolution at high total protein concentrations whereas cyanide reduction is less favored over H_2 evolution at high total protein concentrations. All three steady-state observations can be explained by a model whereby cyanide is proposed to bind to a redox state of the MoFe protein more oxidized than that reactive toward H_2 evolution and N_2 reduction. To test this model, we have examined the pre-steady-state kinetic behavior of both cyanide reduction by *A. vinelandii* nitrogenase and cyanide inhibition of total electron flow through nitrogenase. The data show that in the presence or absence of cyanide there is a short lag of 100 ms before H_2 is detected, followed by a linear phase of H_2 evolution lasting for about 3 s, during which time no effects of cyanide are observable. After 3 s electron flow is finally inhibited by cyanide, and the cyanide reduction product CH_4 is finally formed. These delays are dramatically greater than expected on the basis of the current understanding of the mechanism of nitrogenase. These steady-state and pre-steady-state cyanide data can be simulated, however, by a new scheme that involves cyanide binding to a single site on nitrogenase and inducing an initial modification of the enzyme via a slow step, which must occur prior to cyanide reduction or inhibition.

Molybdenum nitrogenase is comprised of two proteins, the molybdenum–iron protein (MoFe protein) and the iron protein (Fe protein). Nitrogenase turnover requires these two proteins, a low potential reductant (sodium dithionite in vitro), Mg-ATP,[1] protons, and an anaerobic environment (Bulen & LeComte, 1966). The direction of electron flow through nitrogenase has been extensively studied, and the steps involved have been recently reviewed (Thorneley & Lowe, 1985). The Fe protein, with two molecules of MgATP bound, forms a complex with the MoFe protein. Within the complex a single electron is transferred from the Fe protein to the MoFe protein concomitant with the hydrolysis of the two molecules of MgATP. The complex then dissociates (Hageman & Burris, 1987a,b, 1979) in what is usually the rate-limiting step in nitrogenase turnover (Thorneley & Lowe, 1983), yielding free oxidized Fe protein with two MgADP molecules bound. The Fe protein is then rereduced with two MgADPs being replaced by two MgATPs on the reduced Fe protein (Ashby & Thorneley, 1987).

Nitrogenase catalyzes the six-electron reduction of dinitrogen to ammonia, the two-electron reduction of protons to form hydrogen gas, and the reduction of a large number of alternative substrates involving 2–14 electrons (Burgess, 1985). Because no nitrogenase substrate is completely reduced by only one electron, the enzyme must go through more than one catalytic cycle before products can appear. This leads to the concept that there are different redox "states" of the MoFe protein present during turnover. Here we will use the nomenclature shown in Scheme I to describe those states where E_0 = $^1/_2$ MoFe protein in its dithionite-reduced state (Thorneley & Lowe, 1985) and where each arrow represents a single catalytic cycle, involving a rate-determining step, k_1, as described above.

Scheme I

$$E_0 \xrightarrow[k_1]{+e^-} E_1 \xrightarrow[k_1]{+e^-} E_2 \xrightarrow[k_1]{+e^-} E_3 \xrightarrow[k_1]{+e^-} \text{etc.}$$

Both steady-state (Burgess, 1985; Ashby et al., 1987) and pre-steady-state (Thorneley & Lowe, 1985) kinetic data have been interpreted in terms of different substrates and inhibitors binding to different redox states of the MoFe protein. For steady-state experiments it is generally accepted that increasing the ratio of the Fe protein to the MoFe protein favors the formation of the more highly reduced states of the substrate-reducing MoFe protein (Davis et al., 1975; Hageman & Burris, 1980; Wherland et al., 1981). For N_2 fixation

† This work was supported at UC Irvine by USDA–Competitive Grants Organization 85-CRCR-1-1635 and by a NATO grant to B.K.B., R.N.F.T., and D.J.L.

* To whom correspondence should be addressed at the Department of Molecular Biology and Biochemistry, University of California.

‡ Agriculture Food Research Council Institute of Plant Science Research, University of Sussex.

§ Department of Molecular Biology and Biochemistry, University of California.

∥ Supported in part by a National Institutes of Health predoctoral training grant.

[1] Abbreviations: ATP, adenosine 5′-triphosphate; Tes, *N*-[tris(hydroxymethyl)methyl]-2-aminoethanesulfonic acid; Hepes, 4-(2-hydroxyethyl)-1-piperazineethanesulfonic acid. The word "cyanide" is used when we are unable to distinguish between the two species HCN and CN^- that are both present in solution at significant concentrations over the pH range used.

0006-2960/89/0428-8460$01.50/0

experiments, a number of investigators have observed that increasing the Fe protein:MoFe protein ratio causes a shift in electron allocation away from H_2 evolution and into N_2 reduction (Silverstein & Bulen, 1970; Davis et al., 1975; Wherland et al., 1981). In contrast, for cyanide (Li et al., 1982), CH_3NC (Rubinson et al., 1983), and HN_3 (Dilworth & Thorneley, 1981; Rubinson et al., 1985), the trend is in the opposite direction, with H_2 evolution being favored over the six-electron reductions of cyanide, CH_3NC, or NH_3 at high Fe protein:MoFe protein ratios. These results have been explained by suggesting that the alternative substrates cyanide, CH_3NC, and NH_3 bind to the resting E_0 state, of the MoFe protein while H_2 evolution and N_2 binding occur at the more reduced states, E_2 and E_3, respectively (Burgess, 1985; Thorneley & Lowe, 1985). This interpretation is also consistent with the additional observation that the alternative substrates cyanide (Li et al., 1982), CH_3NC (Rubinson et al., 1983), and HN_3 (Rubinson et al., 1985) eliminate the H_2 evolution reaction when they are present in infinite concentrations whereas N_2 cannot (Hadfield & Bulen, 1969; Simpson & Burris, 1984).

The technique of pre-steady-state acid quench of active nitrogenase and subsequent chemical analysis for products have the potential to provide much more specific information concerning the states of the MoFe protein that bind different substrates than does conventional steady-state kinetic analysis. The current interpretation of the available pre-steady-state data is that every catalytic cycle of electron transfer between the Fe protein and the MoFe protein involves the same rate-limiting protein–protein dissociation step with $k = 6.4\ s^{-1}$ at 23 °C, and thus, the transitions from E_0 to E_1, from E_1 to E_2, etc. each occur at the same rate (Thorneley & Lowe, 1983, 1985). It is therefore possible to determine how many catalytic cycles have occurred prior to the release of a specific reduction product. This information has been obtained from pre-steady-state data on H_2 evolution and N_2 reduction (Thorneley & Lowe, 1985). By making the assumptions that the number of catalytic cycles needed depended upon (a) the number of electrons required for a particular reaction and (b) the redox state of the MoFe protein reactive toward that substrate, it was then possible to determine which redox state of the MoFe protein is reactive toward H_2 evolution and N_2 binding. The pre-steady-state data have thus been interpreted to show H_2 evolution occurring at state E_2 (as well as at more reduced states) and N_2 binding occurring at states E_3 and E_4 (Thorneley & Lowe, 1985). This interpretation is fully consistent with the steady-state data discussed above.

In the present study we have examined the pre-steady-state kinetics of the six-electron reduction of cyanide to $CH_4 + NH_3$. This substrate was chosen because its steady-state kinetic behavior differs markedly from that of N_2 reduction, leading to the prediction that it binds to state E_0 (Burgess, 1985). However, due to the pK_a of HCN (9.11 at 30 °C) a solution of NaCN at a pH in the range of 6–9 contains significant amounts of both HCN and CN^-. Li et al. (1982) obtained evidence that HCN is the substrate for nitrogenase whereas CN^- is a reversible inhibitor of total electron flow through the enzyme. In addition, physical evidence for CN^- binding to the dithionite-reduced state of isolated FeMoco has been obtained (Smith et al., 1985; Burgess et al., 1987), suggesting that it binds to the resting E_0 state of the enzyme.

Materials and Methods

Reagents and Chemicals. ATP,[1] creatine phosphokinase, creatine phosphate, Tes,[1] and Hepes[1] were from the Sigma Chemical Co. $Na_2S_2O_4$ was from E-M Chemicals (a division of E. Merck). NaCN was from BDH Chemicals.

Nitrogenase. The *Azotobacter vinelandii* MoFe protein (*Av*1) and Fe protein (*Av*2) were purified and analyzed as described elsewhere (Burgess et al., 1980). Specific activities of the proteins were 1720 nmol of $H_2\ min^{-1}$ (mg of *Av*2)$^{-1}$ and 2720 nmol of $H_2\ min^{-1}$ (mg of *Av*1)$^{-1}$. Steady-state assays for these proteins with cyanide were performed and analyzed as described previously (Li et al., 1982) except that products were measured with a Varian 3700 gas chromatograph with a Poropak N column (He) and a flame ionization detector for CH_4 analysis and a thermal conductivity detector with a molecular sieve 13X column (Ar) for H_2 analysis. Ammonia was determined by an HPLC fluorescence method described elsewhere (Corbin, 1984).

Pre-Steady-State Experiments. Rapid chemical quench was performed at 23 °C as described by Lowe and Thorneley (1984), modified by using an all glass syringe, fitted with a gas-tight rubber closure, to contain the quenching agent. A total of 0.4 mL of protein–substrate solution was shot into 0.5 mL of 1 M $HClO_4$ with a gas space of 1 mL of Ar. The use of a syringe enables a small volume of gas over the liquid phase to be kept at atmospheric pressure throughout the quenching and gas sampling operations. This procedure eliminates errors due to large changes in pressure, so that small gas volumes can be used, reducing the dilution of gaseous products and increasing the sensitivity of the measurements. A 0.1 M NaCN stock solution was made up in degassed 50 mM Hepes–NaOH buffer, pH 7.5, and was adjusted to pH 7.4 by adding an amount of degassed 1 M HCl determined on a separate aerobic aliquot. Product H_2 in the aqueous phase prior to quenching was measured as described previously (Lowe & Thorneley, 1984); CH_4 was measured as described for C_2H_4 by Lowe and Thorneley (1984).

Computing was done on a MicroVax II computer using National Algorithms Group (NAG) subroutine DO2BAF to solve the differential equations describing the various reaction schemes described under Discussion.

Results

Nitrogenase Turnover Rate Decreases as Protein Concentration Increases. Because of the small quantities of products formed in pre-steady-state kinetic experiments, they must be performed at much higher protein concentrations than steady-state experiments. For *Klebsiella pneumoniae*, Thorneley and Lowe (1984) have shown that the total electron flux through nitrogenase decreases as the total protein concentration increases. Figure 1 shows that the same is true for the *A. vinelandii* nitrogenase used for this study.

Product Distribution as a Function of Protein Concentration. The reduction of the physiological substrate N_2 is known to be favored over H_2 evolution at high ratios of Fe protein to MoFe protein (Silverstein & Bulen, 1970; Davis et al., 1975; Wherland et al., 1981). Recently, Lowe and Thorneley (1984) have developed a comprehensive scheme to explain the mechanism of nitrogenase action which predicts that increasing the total protein concentration at a constant ratio of Fe protein:MoFe protein should have the same effect on electron allocation as increasing the component protein ratio. Thus, N_2 reduction is favored over H_2 evolution at high total protein concentrations (Thorneley & Lowe, 1985). This contrasts with the behavior of cyanide in that high Fe protein:MoFe protein ratios favor H_2 evolution over cyanide reduction (Li et al., 1982). The data in Figure 2 for *A. vinelandii* nitrogenase show that increasing the total protein concentration also favors H_2 evolution over the six-electron reduction of cyanide to $CH_4 + NH_3$.

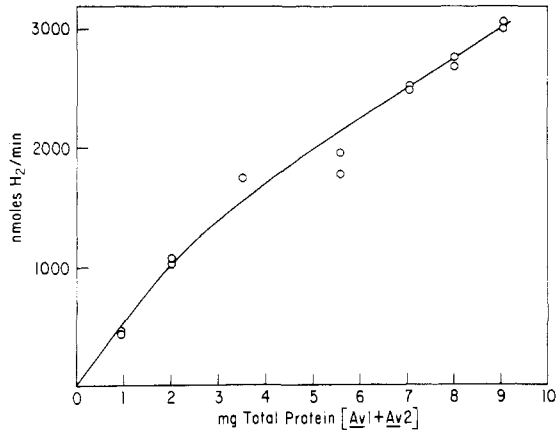

FIGURE 1: Rate of H_2 evolution by nitrogenase as a function of increasing total protein concentration at a fixed molar ratio of 3.9 *Av*2:*Av*1 in 1-mL assays based on molecular weights of 64000 (*Av*2) and 230000 (*Av*1). Reaction times were 5 min (1 mg), 2.5 min (2 mg), 1.5 min (3.5 mg), 60 s (5.6 mg), 45 s (7 mg), 38 s (8 mg), 34 s (9 mg), and 30 s (10 mg). This experiment was performed under an atmosphere of Ar in the absence of any reducible substrates other than protons.

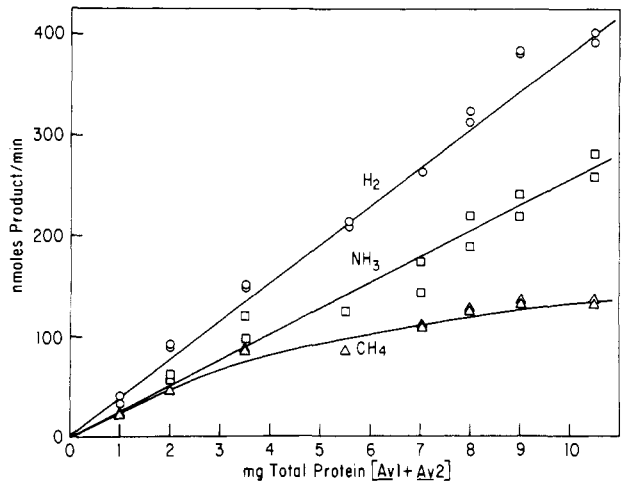

FIGURE 2: Rate of product formation by nitrogenase in the presence of 5 mM NaCN as a function of increasing total protein concentration at a fixed molar ratio of 3.9 *Av*2:*Av*1. Reaction times were as described in the legend to Figure 1.

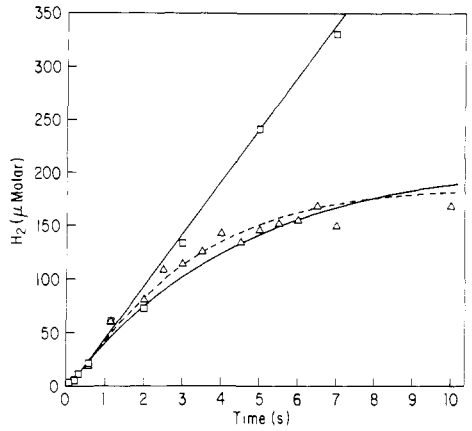

FIGURE 3: Pre-steady-state time courses for H_2 evolution under Ar at 23 °C at pH 7.4 in the presence and absence of cyanide. The data were obtained by the rapid quench technique. Before mixing the syringes contained (A) 57 μM *Av*1, 320 μM *Av*2, 10 mM $MgCl_2$, 1 mM $Na_2S_2O_4$, and 25 mM Hepes buffer, pH 7.4, and (B) 18 mM ATP, 10 mM $MgCl_2$, 20 mM $Na_2S_2O_4$, and 25 mM Hepes buffer, pH 7.4. Points marked with a △ contained 10 mM NaCN in syringe B; points marked with a □ did not. The solid curves are simulations using Scheme III with $k_1 = 5.8\ s^{-1}$ and $k_2 = 0.55\ s^{-1}$, and the dotted curve assumes two slow steps, both with $k_2 = 1.25\ s^{-1}$.

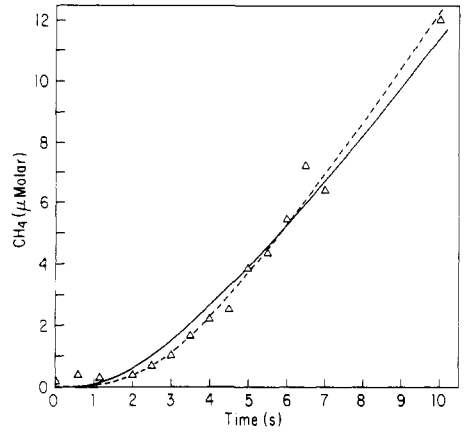

FIGURE 4: Pre-steady-state time course for CH_4 evolution from cyanide under Ar at 23 °C at pH 7.4. Conditions were as for Figure 2 with 10 mM NaCN present in syringe B. The solid curve is a simulation using Scheme III with $k_1 = 5.8\ s^{-1}$ and $k_2 = 0.55\ s^{-1}$, and the dotted curve assumes two slow steps, both with $k_2 = 1.25\ s^{-1}$.

Li et al. (1982) have previously shown that during cyanide reduction the ratio of NH_3 to CH_4 is greater than the anticipated 1:1 with the excess NH_3 arising from a two-electron reduction process (Li et al., 1982). The data in Figure 2 show that the ratio of excess NH_3 to CH_4 is very dependent upon the total protein concentration with high concentrations favoring the formation of excess NH_3. As was the case for the H_2 evolution under Ar reaction shown in Figure 1, an increase in total protein concentration also causes a decrease in turnover rate for a cyanide reduction system. Interestingly, this decrease in electron flow is almost entirely at the expense of the six-electron reduction of HCN to NH_3 and not at the expense of either H_2 evolution or the two-electron reduction of cyanide to produce excess NH_3.

Pre-Steady-State Kinetics in the Presence of Cyanide. Figure 3 shows a plot of H_2 formation by *A. vinelandii* nitrogenase during the first 10 s of turnover under Ar in the absence and presence of 5 mM NaCN. There is a short lag of 100 ms before H_2 is detected in both experiments, as was previously described for the *K. pneumoniae* protein under Ar in the absence of added substrates (Lowe & Thorneley, 1984). This short lag is followed by a linear phase, lasting for about 3 s, during which time no effect of cyanide is observable. After 4 s, the rate of H_2 formation in the presence of cyanide has fallen to its steady-state rate where H_2 evolution is almost eliminated because of the inhibition of total electron flow and the diversion of electrons into cyanide reduction. The final rate of H_2 evolution per milligram of *Av*1 in the absence of cyanide in Figure 3 at 17 mg/mL total protein concentration is 70% of that at 9 mg/mL total protein concentration in Figure 1, consistent with the specific activity continuing to fall as the protein concentration increases.

The corresponding data for CH_4 formation in the presence of cyanide, on the same samples as in Figure 3, are plotted in Figure 4. In this case there is a lag of about 3 s before CH_4 formation is observed. The data shown in Figures 3 and 4 are measured after turnover is initiated by mixing *Av*1 and *Av*2 in one syringe with MgATP plus cyanide in the second syringe. However, similar results were obtained when the proteins were preincubated with cyanide for 30 min prior to the start the reaction with MgATP. Since H_2 evolution (Figure 3) and CH_4 evolution (Figure 4) are linear after the initial burst and lag phases, there can be no significant effect of accumulation of products or exhaustion of substrates.

Scheme II

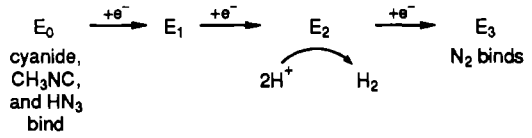

Discussion

The steady-state kinetic behavior of the six-electron reduction of N_2 by nitrogenase differs markedly from the six-electron reductions of the alternative substrates cyanide, CH_3NC, and HN_3 in two important ways. First, on extrapolation to infinite concentrations of cyanide, CH_3NC, and HN_3, the H_2 evolution reaction is almost completely suppressed (Li et al., 1982; Rubinson et al., 1983, 1985) whereas at extrapolate infinite concentrations of N_2, H_2 evolution continues (Hadfield & Bulen, 1969; Simpson & Burris, 1984). Second, as the ratio of the Fe protein to the MoFe protein is increased, the reduction of N_2 becomes favored over H_2 evolution (Silverstein & Bulen, 1970; Davis et al., 1975; Wherland et al., 1981), whereas the reductions of cyanide, CH_3NC, and HN_3 become less favored relative to H_2 evolution (Li et al., 1982; Rubinson et al., 1983, 1985). The data in Figure 2 extend these steady-state experiments to include a third observation, that the six-electron reduction of cyanide is less favored over H_2 evolution at high total protein concentration. Again this behavior is the opposite of N_2 reduction, which is favored over H_2 evolution at high total protein (Thorneley & Lowe, 1985).

All three of the above steady-state observations can be explained by a model of the type shown in Scheme II, which suggests that different substrates bind to different redox states of the MoFe protein. Increasing the ratio of the Fe protein to the MoFe protein or increasing the total protein concentration would both tend to reduce the amount of E_0 available and favor the formation of the more reduced states E_2 and E_3. This scheme is therefore consistent with the observations that N_2 is favored over H_2 evolution which is favored over cyanide reduction as the Fe:MoFe protein ratio or total protein concentration is increased.

It is important to note that Scheme II makes predictions only about when cyanide or N_2 might bind, not about what happens subsequently when a steady state has been achieved. The six-electron reduction of cyanide to CH_4 and NH_3 appears to occur via the formation of a two-electron reduced, enzyme-bound intermediate, which can be hydrolyzed to yield excess NH_3 and HCHO (Li et al., 1982). We would therefore predict that once cyanide is bound, any conditions that would slow the turnover rate of the MoFe protein would increase the lifetime of cyanide reduction intermediates and, thus, increase the likelihood that an intermediate could be hydrolyzed if this can occur at any point in the overall kinetic cycle. This agrees with the observation of Li et al. (1982) that low ratios of Fe:MoFe protein, which slow the turnover rate of the latter, decrease the proportion of bound cyanide that goes on to be reduced by six electrons and increase the proportion that is hydrolyzed at the two-electron level. Figure 1 shows that as the total protein concentration is increased, the turnover rate of nitrogenase decreases, which again should increase the lifetime of cyanide reduction intermediates. The data in Figure 2 are consistent with this view. They show a dramatic decrease in the proportion of cyanide that goes on to be reduced by six electrons and a corresponding increase in the formation of the two-electron product excess NH_3 as the total protein concentration is increased.

The steady-state kinetic data just discussed strongly support the idea that cyanide binds to a redox state of the MoFe protein more oxidized than that reactive toward H_2 evolution or N_2 reduction, most probably to the E_0 dithionite-reduced state. NaCN solutions also contain CN^-, which Li et al. (1982) proposed to be a reversible inhibitor of electron-flow-through nitrogenase. The mechanism of Thorneley and Lowe (1985) predicts that, for pre-steady-state experiments, the factors that affect the length of lag times should be (1) the oxidation level of the MoFe protein to which a substrate or inhibitor binds and (2) the number of electron transfers (rate-limiting steps) required to reduce that substrate to products. In fact, with these criteria, the Thorneley and Lowe (1985) mechanism accurately predicted the pre-steady-state lag times for H_2 evolution and NH_3 production during N_2 fixation by nitrogenase.

If we apply these same criteria, we can make very specific predictions concerning the pre-steady-state lag times for cyanide reduction and inhibition of electron flow. Thus, if the inhibitor binds to a more oxidized state of the MoFe protein than the one that evolves H_2, there should be no delay before inhibition of total electron flow is observed. If the substrate also binds to state E_0, there should be a delay of ca. 500 ms before the six-electron reduction product, CH_4, is formed (Thorneley & Lowe, 1985). The data in Figures 3 and 4 conclusively demonstrate that the delays occurring before total electron flow is inhibited or CH_4 is produced are dramatically greater than can be predicted by the above criteria. Indeed these delays are equivalent to the time required for 18–20 electron-transfer/protein-dissociation cycles. We consider this number to be too large to have any significant mechanistic interpretation and conclude that some additional slow process(es) must occur before cyanide reduction or inhibition of electron flow can take place.

Another important aspect of the pre-steady-state data is the close similarity between the lags before CH_4 forms and before H_2 formation is inhibited. Li et al. (1982) found that the apparent K_m of HCN as substrate and the apparent K_I of CN^- as inhibitor were differnt by a factor of 165 and assumed no connection between the binding of HCN and CN^-. Later the two species were proposed to bind independently, in productive and nonproductive modes, to the same site (Burgess, 1985). If that independent binding model is correct, however, it is difficult to understand why HCN reduction and CN^- inhibition exhibit indistinguishable pre-steady-state lag times (Figures 3 and 4). A simpler interpretation is that the same process is responsible for both lags. We suggest that this process involves cyanide binding to a single site and inducing an initial modification of the enzyme via a slow step. This modification must take place before any cyanide inhibition or reduction can occur.

A reaction scheme summarizing this, using the mechanism of Thorneley and Lowe (1985), is shown in Scheme III, where E represents unmodified enzyme and *E indicates enzyme that has undergone initial, cyanide-induced, modification. In this scheme, the species with unprotonated cyanide bound are incapable of further reduction, whereas the species with protonated cyanide can be reduced as indicated by Li et al. (1982). To make this scheme consistent with the apparent difference in binding constants between CN^- and HCN, the pK_a of bound cyanide must be much lower than that of free cyanide (coordination of a ligand to a metal invariably decreases the pK_a). As shown in Figures 3 and 4, this scheme can simulate our pre-steady-state H_2 and CH_4 formation data. Additional slow steps, each with the same rate constant, give simulations that

Scheme III: Proposed Scheme for Cyanide Interaction with Nitrogenase Involving a Cyanide-Dependent Modification of the Enzyme (from E to *E) Which Occurs in a Slow Process[a]

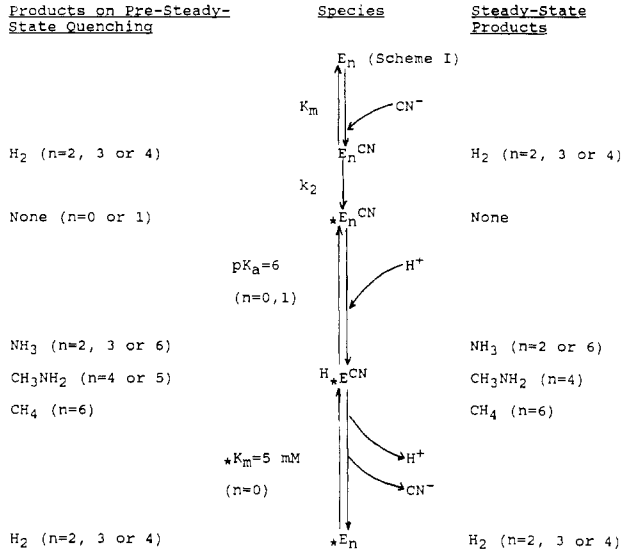

[a] This scheme was used to simulate the data shown in Figures 3–6. CN^- binding was arbitrarily chosen for this illustration; however, the data are unable to distinguish which species, CN^- or HCN, actually binds.

improve the fit marginally by giving a sharper cutoff in H_2 formation and onset of CH_4 formation. The dotted lines in Figures 3 and 4 show this for two slow steps. Liang and Burris (1988) have recently published a time course for H_2 evolution from *A. vinelandii* nitrogenase in the presence of NaCN, showing a sharp onset of inhibition of H_2 evolution after ca. 10 s. Their conditions are very different from ours as they used an unsaturating Fe protein:MoFe protein of 1.23:1 that gives intrinsically long lags. This makes analysis of their data in terms of our Scheme III impossible since under conditions of nonsaturating electron flux a detailed knowledge of the rate constants that define the Fe protein cycles (Lowe & Thorneley, 1984) is required. Under our conditions, with a saturating component protein ratio, simulations are possible because the kinetics are determined by k_1 (Scheme I), which was determined from the steady-state rate of H_2 evolution in the absence of cyanide.

In addition to accurately predicting the pre-steady-state behavior of cyanide, the model shown in Scheme III also offers new insight into the steady-state effects of cyanide. For example, the independent CN^-/HCN binding hypothesis (Li et al., 1982) requires that as the cyanide concentration approaches infinity, the total electron flux approaches zero. In contrast, Scheme III requires zero H_2 evolution at infinite cyanide but a constant rate of cyanide reduction dependent on the ratio of unprotonated to protonated bound cyanide (i.e., at high pH this constant rate should be lower). In order to further evaluate Scheme III, we have, therefore, reexamined the supplementary tables of data presented by Li et al. (1982) where steady-state information on inhibition at higher CN^- concentrations than that shown in Figure 2a of that paper is given. These data are shown in Figure 5, together with simulations using Scheme III at the appropriate pHs as well as the K_I = 27.2 μM CN^- curve (dotted) predicted by the independent CN^-/HCN model of Li et al. (1982). As shown in Figure 5, the data show small, but significant, systematic deviations from the ideal, hyperbolic K_I curve, and the deviations are dependent on pH in exactly the way to be expected from Scheme III. Figure 6 further shows the corresponding product formation curve with steady-state data from the

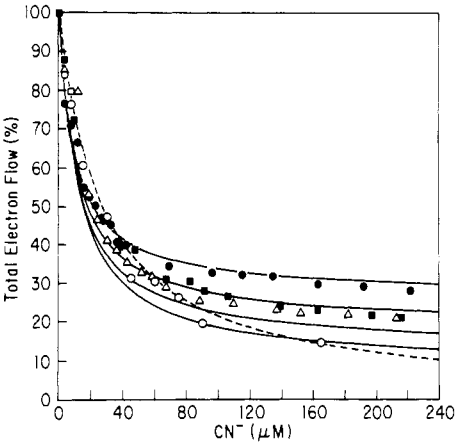

FIGURE 5: Steady-state inhibition of total electron flux by cyanide. The data are from supplementary tables I–IV of Li et al. (1982) (cf. their Figure 2a): (●) pH 7.1, (△) pH 7.3, (■) pH 7.5, and (○) pH 7.7. The solid curves are simulations using Scheme III with k_1 = 7.2 s^{-1}. The dotted curve is for competitive inhibition with K_I = 27.2 μM CN^-.

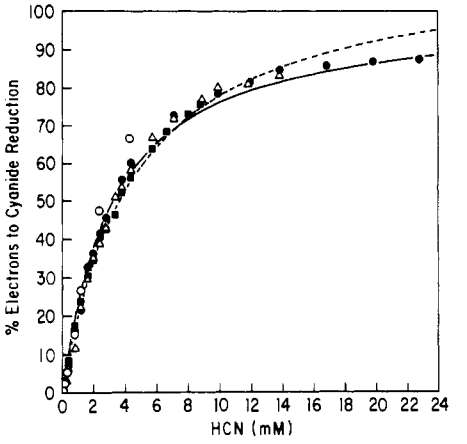

FIGURE 6: Steady-state precentage of electron flux into cyanide reduction. The data are from Li et al. (1982) (cf. their Figure 5) as described in Figure 5, with the solid line simulated using Scheme III. The dotted curve is for K_m = 4.5 mM HCN and V_{max} = 113%.

supplementary tables describing Figure 5 of Li et al. (1982). The solid line in Figure 6 is simulated with Scheme III and is independent of pH, and the dotted line is a K_m = 4.5 mM HCN curve with V_{max} = 113% as described by Li et al. (1982).

It is important to note that the *three* variables, apparent K_m for HCN, apparent K_I for CN^-, and fraction of electron flux remaining at high cyanide (at several pHs), are successfully simulated from Scheme III by using only *two* unknown parameters, namely, (1) the cyanide binding constant ($*K_m$ of Scheme III) and (2) the pK_a of bound cyanide. These parameters were estimated from the values required to give good simulations in Figures 5 and 6. The only additional parameter used was (3) a value for k_1, the rate-limiting step in overall turnover, that we calculated from the overall turnover rate at the appropriate temperature.

The pre-steady-state simulations of Figures 3 and 4 are affected by the same parameters as the steady-state simulations given above plus (4) the binding constant, K_m (Scheme III), of cyanide to E_n, (5) the rates of H_2 release from the various E_n and E_n^{CN} species, (6) k_2, the slow interconversion step from E_n^{CN} to $*E_n^{CN}$, (7) the number of species E_n that can bind cyanide, and (8) the number of species E_n^{CN} capable of conversion to $*E_n^{CN}$. The values used in the simulations of Figures 3 and 4 were chosen arbitrarily from within the range of those giving good simulations. The fits shown in Figures 3 and 4

Scheme IV: Possible Mechanism for Cyanide Binding to Nitrogenase Involving Ligand Replacement, Inhibition of Total Electron Flow by Bound CN^-, and Proton-Induced Reduction To Ultimately Give the Products CH_3NH_2, $CH_4 + NH_3$, and $HCHO + NH_3$[a]

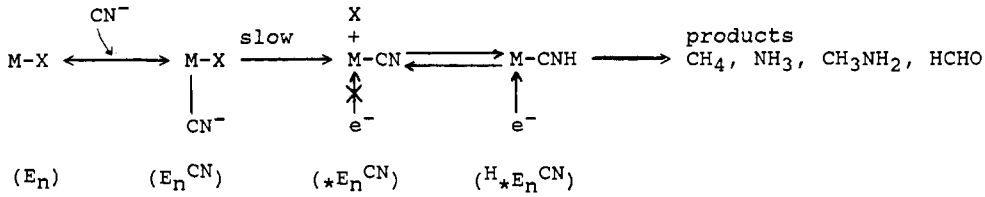

[a] Electron transfer to M–CNH may be directly from the Fe protein to the FeMo cofactor or within the MoFe protein from another center such as a "P" cluster. The dissociation of ligand X is a "once only" activation step which does not occur in subsequent catalytic cycles and which requires at least one electron to have been transferred from the Fe protein to the MoFe protein.

can be improved by introducing more variables, but these fits are not presented because they may be overinterpretations of the data. However, when the large number of simulations of the pre-steady-state data of Figures 3 and 4 that we have done is combined with the three features of the pre-steady-state simulations that are directly measurable, namely, the length of the lag before H_2 evolution is inhibited, the length of the lag before CH_4 formation is observed, and the sharpness of onset of the inhibition of H_2 evolution, we are able to draw some mechanistic conclusions. For example, rate constants for k_2 of less than 0.5 s^{-1} always produce too long a lag, and rate constants of greater than 7 s^{-1} always produce too short a lag, independent of the values chosen for the other parameters. It is also essential to include H_2 formation from both E_n and E_n^{CN} in Scheme III; otherwise, the onset of inhibition of H_2 evolution is insufficiently sharp. Unfortunately, this type of analysis cannot answer more specific chemical questions so that we cannot say which or how many of the species E_n^{CN} undergo the slow step or whether CN^- or HCN actually binds. In addition, we cannot say whether cyanide binds to nitrogenase through C or N, or which of these atoms are protonated, although studies of CN^- binding to reduced Mo centers favor binding through carbon (Pombeiro et al., 1986).

Scheme III can be used to explain the steady-state and pre-steady-state data on cyanide reduction by and cyanide inhibition of nitrogenase. This scheme is a modification of the mechanism of Thorneley and Lowe (1985) involving the following additional assumptions: (1) there is an initial, cyanide-induced slow step that modifies the enzyme (E_n^{CN} to $^*E_n^{CN}$); (2) cyanide binds rapidly and reversibly to a single site on the enzyme; (3) when bound cyanide is protonated, it is reduced to $NH_3 + HCHO$, CH_3NH_2, and $NH_3 + CH_4$ at the two-, four-, and six-electron reduced states of the modified enzyme; and (4) when bound cyanide is not protonated, it prevents electron transfer from the Fe protein to the MoFe protein of nitrogenase. Assumptions 3 and 4 are derived from Li et al. (1982), and assumption 2 is consistent with the proposal that cyanide binds in productive and nonproductive modes to the same site (Burgess, 1985).

Assumption 1 is new, but such a slow process is required to explain the initial long lags. What, then, could this slow process be? It is not part of the normal cycle of steady-state cyanide reduction since it is far too slow. Nor is it a slow activation of the enzyme before turnover can start, since H_2 formation begins after only 50 ms in both the presence and absence of cyanide. One possibility is shown in Scheme IV, which proposes that cyanide binds by replacing a ligand of a metal cluster, a reaction that is slow compared to nitrogenase turnover. A similar scheme involving the replacement of two ligands by two cyanides could also explain the data. By analogy with chemical model systems such a modified cluster would be more difficult to reduce with unprotonated CN^- bound (CN^- is a net electron donor to metal ions, stabilizing the oxidized state); hence, electron transfer to it would be inhibited. However, when the coordinated CN^- is protonated, ease of reduction would be restored and electron transfer switched on. Further support for Scheme IV comes from chemical studies of Hughes et al. (1989), who have recently shown that an {Mo—C≡N} moiety can be reduced in a $2H^+/2e^-$ step to {Mo≡C—NH_2}.

Acknowledgments

We thank Charles Miller for help with the purification of *Azotobacter* nitrogenase.

References

Ashby, G. A., & Thorneley, R. N. F. (1987) *Biochem. J. 246*, 455–465.

Ashby, G. A., Dilworth, M. J., & Thorneley, R. N. F. (1987) *Biochem. J. 247*, 547–554.

Bulen, W. A., & LeComte, J. R. (1966) *Proc. Natl. Acad. Sci. U.S.A. 56*, 979–986.

Burgess, B. K. (1985) in *Molybdenum Enzymes* (Spiro, T., Ed.) pp 161–220, Wiley-Interscience, New York.

Burgess, B. K., Jacobs, D. B., & Stiefel, E. I. (1980) *Biochim. Biophys. Acta 614*, 196–209.

Burgess, B. K., Vaughn, S. A., Conradson, S. B., & Holm, R. H. (1987) *Proc. Int. Conf. Bioinorg. Chem., 3rd*, 307.

Corbin, J. L. (1984) *Appl. Enviror. Microbiol. 47*, 1027–1030.

Davis, L. C., Shah, V. K., & Brill, W. J. (1975) *Biochim. Biophys. Acta 403*, 67–78.

Dilworth, M. J., & Thorneley, R. N. F. (1981) *Biochem. J. 193*, 971–983.

Hadfield, K. L., & Bulen, W. A. (1969) *Biochemistry 8*, 5103–5108.

Hageman, R. V., & Burris, R. H. (1978a) *Biochemistry 17*, 4117–4124.

Hageman, R. V., & Burris, R. H. (1978b) *Proc Natl. Acad. Sci. U.S.A. 75*, 2699–2702.

Hageman, R. V., & Burris, R. H. (1979) *J. Biol. Chem. 254*, 11189–11192.

Hageman, R. V., & Burris, R. H. (1980) *Biochim. Biophys. Acta 591*, 63–75.

Hughes, D. L., Mohammed, M. Y., & Pickett, C. J. (1989) *J. Chem. Soc., Chem. Commun.* (in press).

Li, J.-G., Burgess, B. K., & Corbin, J. L. (1982) *Biochemistry 21*, 4393–4402.

Liang, J., & Burris, R. H. (1988) *Proc. Natl. Acad. Sci. U.S.A. 85*, 9446–9450.

Lowe, D. J., & Thorneley, R. N. F. (1984) *Biochem. J. 224*, 877–886.

Pombeiro, A. J. L., Hughes, D. L., Pickett, C. J., & Richards, R. L. (1986) *J. Chem. Soc., Chem. Commun.*, 246–247.

Rubinson, J. F., Corbin, J. L., & Burgess, B. K. (1983) *Biochemistry 22*, 6260–6268.

Rubinson, J. F., Burgess, B. K., Corbin, J. L., & Dilworth,

M. J. (1985) *Biochemistry 24*, 273–283.
Silverstein, R., & Bulen, W. A. (1970) *Biochemistry 9*, 3809–3815.
Simpson, F. B., & Burris, R. H. (1984) *Science 224*, 1095–1097.
Smith, B. E., Bishop, P. E., Dixon, R. A., Eady, R. R., Filler, W. A., Lowe, D. J., Richards, A. J. M., Thomson, A. J., Thorneley, R. N. F., & Postgate, J. R. (1985) *Proc. Int. Symp. Nitrogen Fixation Res. Prog. 6th*, 597–603.
Thorneley, R. N. F., & Lowe, D. J. (1983) *Biochem. J. 215*, 393–403.
Thorneley, R. N. F., & Lowe, D. J. (1984) *Biochem. J. 224*, 903–909.
Thorneley, R. N. F., & Lowe, D. J. (1985) in *Molybdenum Enzymes* (Spiro, T., Ed.) pp 221–284, Wiley-Interscience, New York.
Wherland, S., Burgess, B. K., Stiefel, E. I., & Newton, W. E. (1981) *Biochemistry 20*, 5132–5140.

Inhibition Kinetics of Acetylcholinesterase with Fluoromethyl Ketones†

Karen N. Allen and Robert H. Abeles*
Graduate Department of Biochemistry, Brandeis University, 415 South Street, Waltham, Massachusetts 02254
Received March 21, 1989; Revised Manuscript Received June 21, 1989

ABSTRACT: A series of trifluoromethyl ketones that reversibly inhibit acetylcholinesterase and pseudocholinesterase were synthesized. By analogy to chymotrypsin and on the basis of data reported here, we propose that the active-site serine adds to the ketone to form an ionized hemiketal. The compound (5,5,5-trifluoro-4-oxopentyl)trimethylammonium bicarbonate (**1**) inhibits acetylcholinesterase with K_i = 0.06×10^{-9} M and pseudocholinesterase with $K_i = 70 \times 10^{-9}$ M. Replacement of the nitrogen of **1** by carbon (compound **2**) increases K_i for **1** 200-fold for acetylcholinesterase but does not significantly alter K_i for pseudocholinesterase. The K_i for the methyl ketone corresponding to **2** is 2×10^{-4} M for both enzymes, as compared with 12×10^{-9} M for the trifluoromethyl ketone (acetylcholinesterase). For both enzymes, a linear decrease in log K_i with decreasing pK of the inhibitor hydrate was observed with ketones containing from 0 to 3 fluorines. We attribute this effect to the stabilization of the hemiketal oxyanion. The reduction of the pK of the hemiketal by the trifluoromethyl group is an important contributing factor to the low K_i of trifluoromethyl ketones. The inhibition of acetylcholinesterase by tetramethylammonium chloride and trifluoroacetone was compared to the inhibition by **1**, which is a composite of the two smaller inhibitors. The entropic advantage of combining the smaller inhibitors into one molecule is 1.1×10^3 M. Inhibitors with $K_i \leq 70 \times 10^{-9}$ M are slow binding (Morrison, 1982; Morrison & Walsh, 1988). The kinetic data do not require formation of a noncovalent complex prior to formation of the ketal, although such a complex(es) cannot be excluded. The hydrate/ketone ratios for trifluoro ketones as well as the rates of hydration and dehydration were measured with an $NADP^+$-dependent alcohol dehydrogenase and were found to be ~500, 0.25 s^{-1}, and 5×10^{-4} s^{-1}, respectively. The ketone, not the hydrate, reacts with the enzyme to form the enzyme–inhibitor complex. For "slow-binding" inhibitors, k_{on}, based on actual ketone concentration, ranges from 10^6 to 10^8 M^{-1} s^{-1}.

Trifluoromethyl ketones are potent inhibitors of acetylcholinesterase (EC 3.1.1.7) (Brodbeck, 1979; Gelb et al., 1987). These compounds also inhibit serine proteases. Trifluoromethyl ketones react with the active-site serine of chymotrypsin and elastase to form an ionized hemiketal as shown in Scheme I (K. D. Brady, D. Ringe, and R. H. Abeles, manuscript in preparation; Takahashi et al., 1988; Liang & Abeles, 1987). The pK of the hemiketal is <4.5 and that of the histidine is >10.5 (T.-C. Liang, K. D. Brady, and R. H. Abeles, manuscript in preparation). It is generally believed that the active-site structure and mechanism of catalysis of the serine proteases and the cholinesterases are similar (Hess, 1971). Inactivation of acetylcholinesterase by the fluorophosphate pinacolyl methylphosphonofluoridate reveals phosphorylation of a single serine on a unique polypeptide sequence, similar to that seen for chymotrypsin (Schaffer et al., 1973). Furthermore, the enzymatic hydrolysis of acetylcholine shows a similar pH dependence to ester hydrolysis by chymotrypsin; i.e., k_{cat}/K_m versus pH gives a bell-shaped curve with apparent pK's of ~6.5 and 10.5 and a flat region from pH 7.0 to 9.0 while k_{cat} has an apparent pK of ~6.5 (Rosenberry, 1975). The mechanism for both enzymes has been proven to proceed via acyl-enzyme formation (Froede & Wilson, 1984; Bentley & Rittenberg, 1954). It is, therefore, likely that the complex formed with trifluoro ketones and acetylcholinesterase has a structure similar to that formed with serine proteases.

Scheme I: Formation of Enzyme–Inhibitor Complex

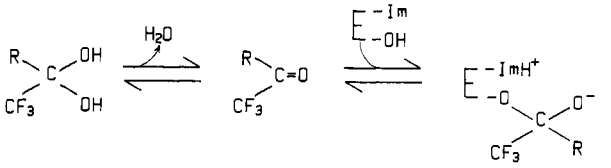

In order to explore the mechanism of inhibition of acetylcholinesterase by trifluoro ketones, we have synthesized a number of fluoromethyl compounds isosteric to acetylcholine

†This work was supported by National Institutes of Health Grant GM12633-28 and by National Science Foundation Grant DMB 85-05498. This is Publication No. 1687 from the Graduate Department of Biochemistry, Brandeis University.
* To whom correspondence should be addressed.

0006-2960/89/0428-8466$01.50/0